Texture parameters of R2* maps are correlated with iron concentration and red blood cells count in clot analogs: A 7-T micro-MRI study

Martin Bretzner, Renaud Lopes, Ray Mccarthy, Delphine Corseaux, Florent Auger, Gillian Gunning, Nicolas Beauval, Antonino Bongiovanni, Meryem Tardivel, Charlotte Cordonnier, et al.

Texture parameters of R2* maps are correlated with iron concentration and red blood cells count in clot analogs: A 7-T micro-MRI study☆

Martin Bretzner [a b], Renaud Lopes [a b], Ray McCarthy [c], Delphine Corseaux [d e f], Florent Auger [a], Gillian Gunning [c], Nicolas Beauval [i], Antonino Bongiovanni [g], Meryem Tardivel [g], Charlotte Cordonnier [h], Jean-Pierre Pruvo [a b], Sophie Susen [d e f], Xavier Leclerc [a b], Grégory Kuchcinski [a b]

[a]Inserm U1171 Degenerative & Vascular Cognitive Disorders, University of Lille, 59000 Lille, France

[b]CHU de Lille, Department of Neuroradiology, 59000 Lille, France

[c]Cerenovus, Neuravi Thromboembolic Initiative, Galway, Ireland

[d]Inserm U1011-EGID, Lille, France

[e]Institut Pasteur de Lille, Lille, France

[f]CHU Lille, Hematology and Transfusion, 59000, Lille, France

[g]Bio imaging center Lille Nord-de-France Campus HU, faculté de médecine, Université de Lille, 59000 Lille, France

[h]CHU de Lille, Department of Neurology, 59000 Lille, France

[i]CHU Lille, Unité Fonctionnelle de Toxicologie, 59000 Lille, France

Highlights

- •RBC count is strongly correlated with iron concentration within clots.
- •Texture analysis of R2* maps predict the RBC count and iron content of clot analogs.
- •R2* maps of RBC rich clots present a more coarse texture.
- •R2* maps of RBC poor clots present a finer texture.

Abstract

Background and purpose

Previous studies have suggested that mechanical revascularization in acute ischemic stroke (AIS) patients could be affected by clot histology. In this 7-T micro-MRI study, we used R2* relaxometry of clot analogs to evaluate the relationship between texture parameters of R2* maps and clot constituents.

Materials and methods

Twelve AIS clot analogs were experimentally generated to obtain a wide range of red blood cell concentrations. All clots underwent a MR acquisition using a 7-T micro-MR system. A 3D multi-echo gradient-echo sequence was performed and R2* maps were generated. First

order and second order statistics of R2* histograms within the clots were calculated. Iron concentration in clots was measured using absorption spectrometry and red blood cell count (RBC) was obtained by histopathological analysis.

Results

RBC count was strongly correlated with iron concentration within clots ($r = 0.87$, $P < .001$). Higher RBC count and iron concentration were significantly correlated with first order parameters including: (a) global positive shift of the R2* histogram with higher '10th percentile', 'median', 'mean' and '90th percentile'; (b) increase of the global magnitude of voxel values with higher 'total energy' and 'root mean squared'; (c) greater uniformity of the voxel values with higher 'uniformity' and lower 'entropy'. Second order statistical parameters confirmed that higher RBC count and iron concentration correlated with (a) greater concentration of high gray-level values in the image; (b) more "coarse" texture of R2* maps.

Conclusions

Texture analysis of MRI-R2* maps can accurately estimate the red blood cell count and iron content of AIS clot analogs.

Graphical abstract

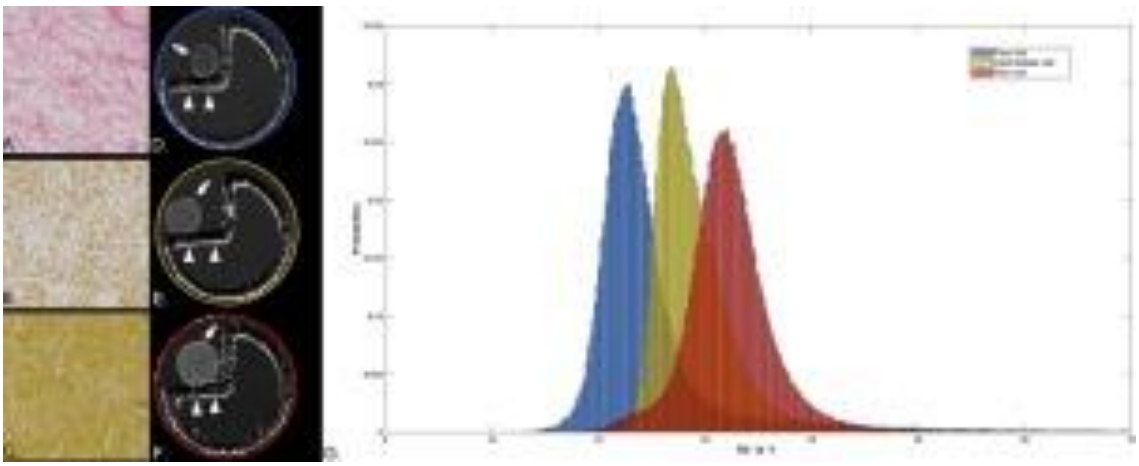

Keywords

MRI

Stroke

Clot

Texture analysis

Relaxometry

Abbreviations

AIS acute ischemic stroke

GLRLM gray-level run length matrix
IV-tPA intravenous thrombolysis
MT mechanical thrombectomy
NETs neutrophils extracellular traps
RBC red blood cell
ROI region of interest
VWF Von Willebrand factor

Introduction

Acute ischemic stroke treatment (AIS) using intravenous thrombolysis (IV t-Pa) and/or mechanical thrombectomy (MT) aims at a quick recanalization of the occluded artery. Despite the improvement of the reperfusion drugs and devices, flow restoration fails to be achieved in 29% of patients resulting in unfavorable clinical outcome [1]. Clots responsible for intracranial occlusions remained unavailable for examination until the recent proliferation of histopathological studies, secondary to MT, provided new insights about their composition. They tend to be heterogeneous and are often classified by the relative composition of two main components, red blood cells and fibrin, the quantities of each are inversely correlated [2]. These constituents have been associated with procedural outcome: RBC-rich clots being easier to retrieve during mechanical thrombectomy and more sensitive to intravenous fibrinolysis [3]. Other thrombus components that play major roles in thrombosis and clot make-up are: platelets, von Willebrand factor (VWF), neutrophil extracellular traps (NETs) and leucocytes. In line with these data, additional reperfusion strategies are being developed. New devices tailored for challenging fibrin-rich clots or clots that are prone to fragmentation are being benchmarked [4]. New drugs, such as ADAMTS-13, a VWF specific protease, or DNAse1 targeting NETs, have been proposed to increase the performance of IV t-Pa [5], [6]. However, to be of most benefit, real-time selection of the optimal recanalization strategy based on histology is needed. As such, histological composition of the clot should be assessed at the time of the diagnosis, during pre-therapeutic imaging. The blooming artifact in MRI, has been attributed to a predominant RBC fraction within clots. However, quantitative methods able to accurately predict the RBC concentration are lacking. R2* relaxometry is a non-invasive method capable of quantifying the MR signal drop related to the presence of paramagnetic substances and R2* values have been linearly correlated with brain iron concentration in post-mortem studies [7]. RBC are iron-rich cells because of the high iron content in hemoglobin, an iron binding protein. Thus, we

hypothesized that R2* relaxometry could quantify iron content within clot analogs and that iron content is correlated with RBC concentration.

Beyond RBC percentage, the study of the spatial distribution of the clot's constituents could provide some clue about its mechanical property or its nature. Texture analysis of MR images is an emerging field in radiology that enables automatic high-throughput extraction of quantitative features of an image that are invisible to the naked eye. Results show promise in predicting histological phenotypes of tumors [8], [9]. Although mostly evaluated in the field of oncology, this approach could help to distinguish histological subtypes of clots.

The aim of the study was to analyze texture parameters of R2* maps of clot analogs on a 7-T micro-MRI and to evaluate their relationship with RBC and iron concentration.

Material and methods

Material

Twelve clot analogs were generated using a previously described methodology to obtain a wide range of RBC concentrations [10]. Briefly, clot analogs of increasing RBC concentrations were formed under static conditions in standing vials using ovine venous blood.

MR acquisitions

All MR acquisitions were performed on a 7-T micro-MR system with a single channel surface coil (BioSpec Brucker, Billerica, Massachusetts, US). A 3D multi-echo gradient-echo sequence was performed using the following parameters: FOV = 16 × 16 × 16 mm; matrix = 128 × 128 × 128, voxel = 0.125 × 0.125 × 0.125 mm; TEs = 7, 14, 21, 28 ms; TR = 50 ms; flip angle = 15°; number of excitations = 7; total acquisition time = 95 min.

All clots were fully immerged into separate vials filled with PBS (phosphate buffer saline 10%) at room temperature (18–22 °C) and leaned on a dedicated support.

Immediately after MR acquisitions, clots were cut into two parts. The first part was frozen at −80 °C for later iron quantification. The second part was fixed into paraformaldehyde for histopathological analysis.

MR imaging analysis

3D R2* maps were automatically generated by a voxel-by-voxel nonlinear least squares fitting of the multi-echo T2*-weighted data 02;witht=echotime,S=measuredsignal,R2∗=transverserelaxationrate, using the open-source Niftyfit toolbox (https://www.cmiclab.cs.ucl.ac.uk/CMIC/NiftyFit-Release). Clots were manually segmented on the R2* maps by a neuroradiologist blinded to iron concentration and RBC count, using the MRIcron software [11].

R2* histograms were computed for each clot using MATLAB (v 2014a, The MathWorks, Natick, 2014).

Texture analysis

First-order and second-order statistical parameters derived from the histograms were calculated using the pyradiomics toolbox [12]. First order parameters described the histograms of voxel intensities using common metrics such as mean, median, variance, skewness, kurtosis, uniformity, entropy, total energy and root mean squared. The second order parameters described the relationship between intensity and spatial distribution. Here, we used Gray Level Run Length Matrix (GLRLM) features and included namely: run percentage, short run emphasis, long run emphasis, low gray level run Emphasis, high gray level run emphasis, run length non-uniformity, run variance, run entropy, gray level non-uniformity and gray level variance. The neighboring window was $3 \times 3 \times 3$. High-quality didactic documentations about GLRLM features are available at: https://www.pyradiomics.readthedocs.io.

Briefly:

- •a run is defined as the length of consecutive pixels that share the same value in a given direction;
- •run percentage describes the number of runs in the region of interest (ROI), a higher percentage indicates a higher number of runs, and a finer texture;
- •short run emphasis measures the distribution of short run lengths, increases with more fine texture;
- •long run emphasis measures the distribution of long run lengths, increases with more coarse texture;
- •low gray level run emphasis measures the distribution of low gray values in the ROI;
- •high gray level run emphasis measures the distribution of high gray values in the ROI;
- •run length non-uniformity measures the heterogeneity of runs in the ROI, a lower value indicate more homogeneity in run lengths;
- •run variance measures the variance in grey intensities for the runs;
- •run entropy describes the randomness in the distribution of run lengths and gray levels, higher values indicate more heterogeneity in texture patterns;
- •gray level non-uniformity measures the homogeneity of gray-level values in the ROI, a lower value indicates a greater similarity in gray levels;
- •gray level variance measures the variance of gray level intensities in runs.

In order to reduce the number of parameters, we analyzed texture using only a single methodology. There are no guidelines regarding the method to use. We hypothesized that GLRLM would be the best suited to evaluate the distribution of RBC along fibrin fibers.

Iron quantification

Clot analogs were accurately weighted and mineralized 25 min at 100 °C with 7.7 mol/L nitric acid solution in ultrapure water, before further iron concentration determination by graphite furnace electrothermal atomic absorption spectrometry (AAnalyst 800, Perkin Elmer, Waltham, USA).

Histopathological analysis

All the samples were fixed in paraformaldehyde, embedded in paraffin and then cut. Slices were stained using Martius Yellow (RBC) and Scarlet Red (Fibrin) then scanned with a digital slide scanner (Axio ScanZ1, Zeiss, Oberkochen, Allemagne). Erythrocytes were automatically counted using a homemade macro on ImageJ based on local maxima filtering [13]. Performance of the automatic count macro was assessed against manual labelling of RBC on a validation subset of 10 microscope fields with an excellent correlation coefficient ($r^2 = 0.91$).

Statistical analysis

Statistical analyses were performed using SPSS 19.0 software (SPSS Inc., Chicago, IL, USA). Quantitative parameters were expressed as median (interquartile range). Three clusters of clots were identified: poor clots with low RBC count (< 0.02 RBC/μm^2) and very low iron concentration (< 10 μg/g), intermediate clots with intermediate-to-high RBC count (0.07–0.11 RBC/μm^2) and intermediate iron concentration (200–500 μg/g), and rich clots with high RBC count (> 0.10 RBC/μm^2) and high iron concentration (> 700 μg/g). Characteristics were compared in the three groups using the Kruskal-Wallis test. Correlations between R2* parameters and (a) iron concentration and (b) RBC count were assessed using Pearson's correlation coefficients (r). Statistical testing was done with α risk levels of 0.05 and 0.01. In order to deal with type 1 error in multiple testing the false discovery rate was calculated and P values were adjusted using the Benjamini and Hochberg method. Data was explored using principal component analysis (PCA) to understand the information provided by the different texture parameters.

Results

Clots main characteristics are presented in Table 1. RBC count was strongly correlated with iron concentration within clots ($r = 0.87$, $P < .001$) as shown in Fig. 1. Illustrative examples of poor, intermediate and rich clots with corresponding R2* histograms are presented in Fig. 2.

Table 1. Characteristics of the clots analogs (n = 12).

Characteristics	**All clots (n = 12)**	**Clot concentration**			
Empty Cell	Empty Cell	**Poor (n = 3)**	**Intermediate (n = 4)**	**Rich (n = 5)**	***Adj P***
Volume (mm^3)	202.7 (110.0–256.1)	91.2 (75.0–96.0)	202.7 (170.0–253.8)	250.1 (217.6–258.0)	.04
Mean R2* (s^{-1})	30.97 (27.03–32.57)	26.63 (25.35–27.16)	29.80 (27.75–31.27)	32.89 (31.60–33.12)	.03
RBC concentration (10^5 cells/mm^2)	9.49 (1.81–11.20)	0 (0–0)	8.03 (7.25–9.50)	11.20 (11.19–11.45)	.02
Iron concentration (µg/g)	420.6 (69.3–854.4)	2.7 (1.9–3.0)	358.0 (302.9–420.6)	859.5 (839.2–899.4)	.02

Data are presented as median (interquartile range). Characteristics of Poor, Intermediate and Rich clots were compared using the Kruskal Wallis test. *P*-values were adjusted for multiple comparisons with the false discovery rate method. RBC: red blood cells.

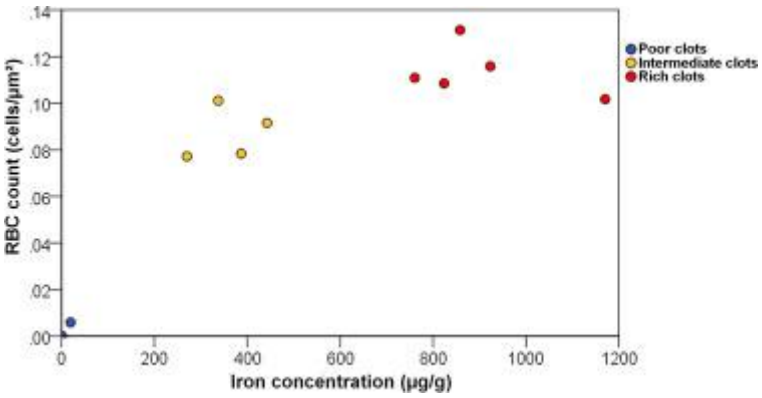

Fig. 1. Dot plot of iron concentration by RBC count in clot analogs. RBC count was linearly correlated to iron concentration (r = 0.87, P < .001). Three clusters were visually observed: poor clots (blue) with low RBC count (< 0.02 RBC/μm^2) and very low iron concentration

(< 10 μg/g), intermediate clots (yellow) with intermediate-to-high RBC count (0.07–0.11 RBC/μm^2) and intermediate iron concentration (200–500 μg/g), and rich clots (red) with high RBC count (> 0.10 RBC/μm^2) and high iron concentration (> 700 μg/g). RBC: red blood cell.

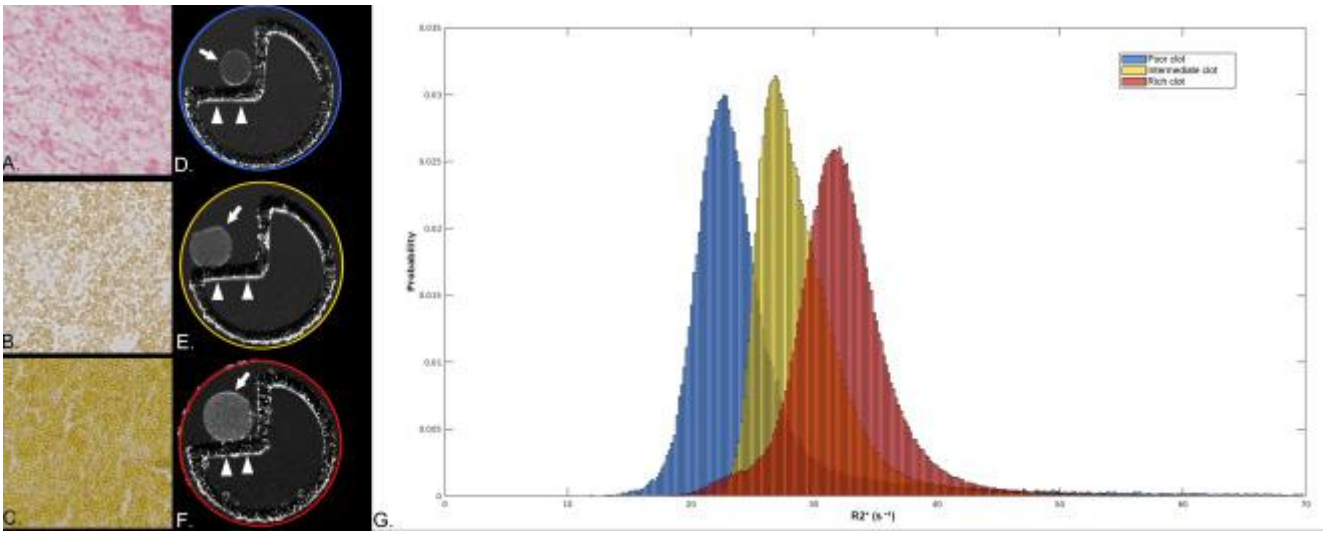

Fig. 2. Illustrative examples of histology, R2* maps and R2* histograms according to clot concentration. Histopathological slices of poor (A, blue), intermediate (B, yellow) and rich (C, red) clots. RBC are stained in yellow (Martius Yellow) and fibrin in red (Scarlet Red). Corresponding R2* maps (D–F, transverse sections) of clots (white arrows) leaned on a dedicated support (white arrow heads) and immerged into vials filled with PBS (phosphate buffer saline 10%) at room temperature (18–22 °C). Corresponding histograms (G) demonstrated a positive shift with concentration increase.

The R2* mean value was positively correlated to the clot's RBC count (r = 0.80, P = 0.02) and iron content (r = 0.79, P = 0.02). Correlations between texture analysis features derived from R2* histograms and maps and (a) iron content and (b) RBC count are presented in Table 2. Higher RBC count and iron concentration were significantly correlated with:

- •a global positive shift of the R2* histogram with higher ‘10th percentile’, ‘median’, ‘mean’ and ‘90th percentile’;
- •an increase of the global magnitude of voxel values with higher ‘total energy’ and ‘root mean squared’;
- •a greater uniformity of the voxel values with higher ‘uniformity’ and lower ‘entropy’.

Table 2. Correlation between texture parameters derived from R2* histograms, iron concentration and RBC count (n = 12).

Texture parameters	**Iron concentration**	**RBC concentration**

Empty Cell	*r*	*Adj P*	*r*	*Adj P*
First order parameters				
R2*_10th percentile	0.84**	.003	0.85**	.004
R2*_Mean	0.79**	.006	0.80**	.009
R2*_Median	0.83**	.003	0.84**	.005
R2*_90th percentile	0.61*	.0497	0.63*	.047
R2*_Variance	−0.32	.34	−0.37	.29
R2*_Skewness	−0.43	.19	−0.47	.17
R2*_Kurtosis	−0.17	.59	−0.26	.43
R2*_Uniformity	0.69*	.02	0.67*	.04
R2*_Entropy	−0.70*	.02	−0.66*	.04
R2*_Total energy	0.83**	.003	0.89**	.002
R2*_Root mean squared	0.76*	.01	0.76*	.02
Second order parameters (GLRLM)				
R2*_Run Percentage	−0.72*	.02	−0.69*	.04
R2*_Short Run Emphasis	−0.69*	.02	−0.49	.14
R2*_Long Run Emphasis	0.84**	.003	0.64*	.046
R2*_Low Gray Level Run Emphasis	−0.84**	.003	−0.69*	.04
R2*_High Gray Level Run Emphasis	0.66*	.03	0.60	.06
R2*_Run Length Non-Uniformity	−0.56	.08	−0.36	.30
R2*_Run Variance	0.79**	.006	0.65*	.04
R2*_Run Entropy	0.84**	.003	0.68*	.04
R2*_Gray Level Non-Uniformity	−0.18	.59	0.07	.84
R2*_Gray Level Variance	−0.49	.13	−0.32	.34

P-values are adjusted the for the false discovery rate using the Benjamini & Hochberg method. **: Result is significant at the 0.01 level. *: Result is significant at the 0.05 level.

Second order features confirmed that higher RBC count and iron concentration correlated with:

- •a greater concentration of high gray-level values in the image (lower ‘low gray level run emphasis’; higher ‘high gray level run emphasis’);
- •a more “coarse” texture of R2* maps (lower ‘run percentage’ and ‘short run emphasis’; higher ‘long run emphasis’).

PCA performed on texture parameters demonstrated that two components were necessary to explain 81% of the variance of the data. The addition of a third component marginally improved the explained variance. The loading plot of the PCA (Fig. 3) showed that 2 families of features could be identified and that second-order parameters provided different information compared to first-order parameters.

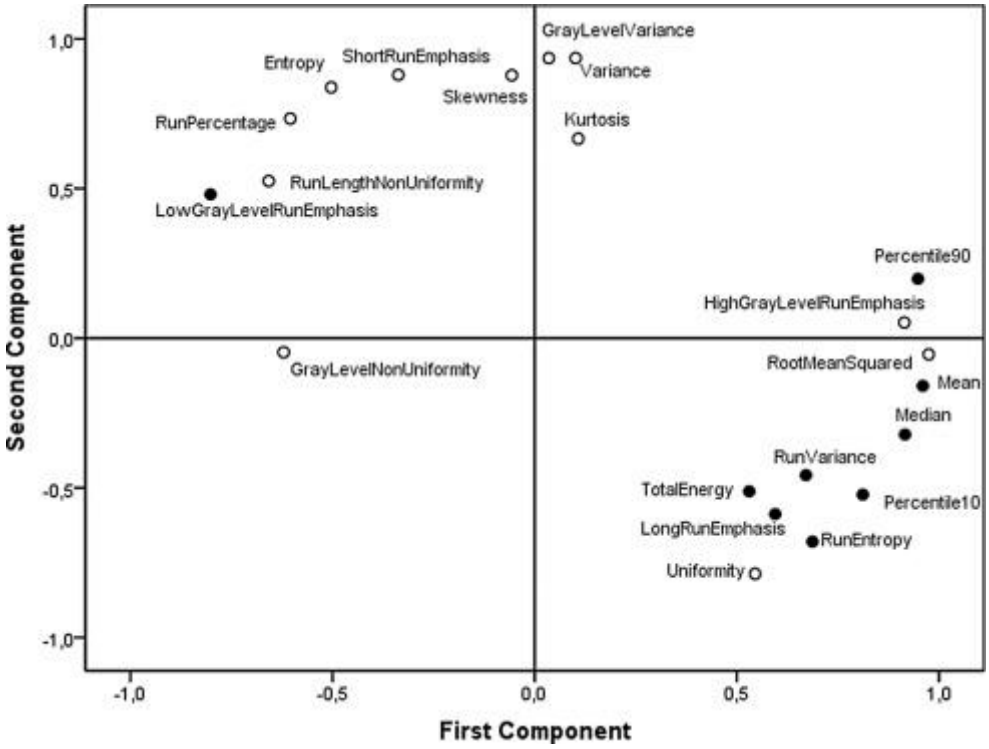

Fig. 3. Loading plot of the principal component analysis performed on texture parameters. The first 2 components of the PCA explain 81% of the variance. First order features GLRLM features significantly correlated with iron concentration or RBC count are marked with a full dot.

Discussion

Using experimental stroke clot analogs, we confirmed the hypothesis that R2* values and texture parameters were linearly correlated with iron content and RBC count. RBC rich clots were associated with higher R2* values and more coarse R2* maps.

This result is in accordance with recent publications of Bourcier et al. [14] and Spencer et al. [15] that showed R2* values could accurately identify RBC rich clots on clinical 1.5 Tesla and 3 Tesla MRI, respectively. The main strength of our study is the use of a 7-Tesla magnetic field. As the main magnetic field increased, the T2* relaxation time would be shorter, and the susceptibility effect of paramagnetic substances would be increased. Another benefit is the increase of the spatial resolution. The blooming artifact on T2* or SWI images is a well-known imaging feature of vessel occlusion in ischemic stroke and has been previously suspected to reflect RBC-rich clots but experimental validation of such hypothesis was lacking [16]. Unlike the quantitative approach we propose, it relies on a binary qualitative evaluation and is not able to depict the broad range of RBC concentrations as revealed by histological studies of clots retrieved during endovascular procedures [2]. R2* mapping also has the advantage of overcoming the variability related to the settings of the acquisition parameters such as the echo time [17].

Histopathological studies also revealed the intra-clot heterogeneity and complexity of the clots retrieved during MT. Beyond clot's main composition (RBC rich vs. RBC poor), the texture analyses performed in this study provide insights about the spatial distribution of the clot's constituents. Although it could seem confusing that RBC rich clots showed both a higher ‘uniformity’ and a more coarse texture on R2* maps, the mathematical meaning is not contradictory. First order parameters such as ‘uniformity’ are calculated from the image histograms and explore intensity values while second order features (GLRLM) provide information about the spatial distribution of those values. A higher ‘uniformity’ means the pixels tend to show similar intensity values through the entire clot and a more ‘coarse’ texture as defined by run length means that the clot consists in larger areas with similar gray level value. In this study, R2* texture analyses showed more long gray level runs in RBC-rich clots and more short gray level runs in fibrin rich clots. According to our findings, clot analogs rich in RBC seemed to be comprised of larger patches of homogeneous texture that could suggest the presence of larger islets of RBC and/or scarcer mesh of fibrin. Among second order features, principal component analysis highlighted ‘low gray level run emphasis’ as a potential discriminator of clot subtype. This parameter was higher in fibrin rich clots and indicated a higher prevalence of contiguous pixels with low intensity values. Fibrin rich clots have been reported to increase friction and thus render retrieval more challenging [18].

Some thrombectomy devices targeted to these challenging clots are being benchmarked and will soon be available for use in clinical practice. As such, prior knowledge of the clot subtype could help plan the procedure and speed up reperfusion. Denorme et al. reported VWF to be inversely correlated to the RBC content in human stroke clots retrieved during MT and showed that the addition of ADAMTS13 to IV t-Pa could reduce the infarct size in a stroke mice model [6]. Boeckh-Behrens et al. found leucocytes to be inversely correlated to the RBC fraction of the clot, and Laridan et al. reported NETs to be co-localized in leucocyte rich portions of human stroke thrombi and showed that adding DNAse1 to IV t-Pa could dissolve stroke clots faster *ex vivo* [19], [20]. Imaging studies of the stroke clot at the acute phase could help by personalizing thrombolysis through adding ADAMTS13 and/or DNAse1 to IV t-Pa, specifically targeting VWF and NETs, improving reperfusion and therefore clinical outcome.

As MRI performance improves, radiologists are able to see more and more hints of the clot histopathology. While our clot analogs were quite homogeneous, real stroke clots are complex, Duffy et al. studied the fragments retrieved per pass of mechanical thrombectomy of stroke patients and reported the first 2 passes to mainly retrieve RBC rich fragments while fibrin rich fragments were more difficult to remove [21]. Texture analysis of real stroke clots would be relevant because of this mixed layout and could help with selection of the most appropriate thrombectomy device prior to the first attempt.

The percentage of RBC and fibrin in clots affects its mechanical properties and response to reperfusion therapy, but another process plays an important part: the clot contraction [22]. This natural process occurs over time as platelets and fibrin fibers form a dense meshwork compressing the erythrocytes into tightly-packed arrays of polyhedrocytes making the clot stiffer and impeding the exchange rate with the external environment [23]. In a recently published study, Tutwiler et al. reported contraction to hamper the rate of fibrinolysis by a 4-fold factor [24]. In the present study we found that fibrin rich clots were significantly smaller than other clots, which could express a more contracted state. Assessing the contracted vs non-contracted state of thrombi at the acute phase of stroke remains for now inaccessible but texture analysis of clot's MRI images could bring some answers in the future.

Our study has several limitations. First, it was designed as a proof of concept study on *ex vivo* stroke clot analogs, which were more homogeneous than *in vivo* human stroke thrombi. Although texture parameters did add some value to the analysis, the association with the RBC count remained stronger with R2* histogram features. Validation of our results on heterogeneous clot analogs and/or real life thrombi is mandatory. High magnetic field MRI

enabled us to acquire images with a 0.125-microns spatial resolution, which is still far from achievable in clinical routine brain MRI. However, experimental studies like this one give direction for further clinical application. Secondly, only 12 clot analogs were analyzed, further validation on a larger sample of human thrombi is needed. Finally, we did not normalize the quantitative features extracted nor tested different neighborhood window sizes, this could hamper results reproducibility.

Conclusions

Texture analysis of MRI R2* maps can accurately quantify the red blood cell count and iron content of in vitro stroke clot analogs. This brings out new neuroimaging biomarkers to improve treatment strategy in acute ischemic stroke.

Funding

This research did not receive any specific grants from funding agencies in the public, commercial or not-for-profit sectors.

Disclosure of interest

R.M. and G.C. are employed by Cerenovus (Gallway, Ireland).

References

[1]
M. Goyal, B.K. Menon, W.H. van Zwam, *et al.*
Endovascular thrombectomy after large-vessel ischaemic stroke: a meta-analysis of individual patient data from five randomised trials
Lancet Lond Engl, 387 (2016), pp. 1723-1731, 10.1016/S0140-6736(16)00163-X

[2]
S.F. De Meyer, T. Andersson, B. Baxter, *et al.*
Analyses of thrombi in acute ischemic stroke: a consensus statement on current knowledge and future directions
Int J Stroke, 12 (2017), pp. 606-614, 10.1177/1747493017709671

[3]
P.A. Brouwer, W. Brinjikji, S.F. De Meyer
Clot pathophysiology: why is it clinically important?
Neuroimaging Clin N Am, 28 (2018), pp. 611-623, 10.1016/j.nic.2018.06.005

[4]
V.S. Fennell, S.V. Setlur Nagesh, K.M. Meess, *et al.*
What to do about fibrin rich ‘tough clots’? Comparing the Solitaire stent retriever with a novel geometric clot extractor in an in vitro stroke model

J NeuroInterventional Surg, 10 (2018), pp. 907-910, 10.1136/neurintsurg-2017-013507

[5]

C. Ducroux, L. Di Meglio, S. Loyau, *et al.*

Thrombus neutrophil extracellular traps content impair tPA-induced thrombolysis in acute ischemic stroke

Stroke, 49 (2018), pp. 754-757, 10.1161/STROKEAHA.117.019896

[6]

F. Denorme, F. Langhauser, L. Desender, *et al.*

ADAMTS13-mediated thrombolysis of t-PA-resistant occlusions in ischemic stroke in mice

Blood, 127 (2016), pp. 2337-2345, 10.1182/blood-2015-08-662650

[7]

C. Langkammer, N. Krebs, W. Goessler, *et al.*

Quantitative MR Imaging of brain iron: a postmortem validation study

Radiology, 257 (2010), pp. 455-462, 10.1148/radiol.10100495

[8]

H.J.W.L. Aerts, E.R. Velazquez, R.T.H. Leijenaar, *et al.*

Decoding tumour phenotype by noninvasive imaging using a quantitative radiomics approach

Nat Commun, 5 (2014), p. 4006, 10.1038/ncomms5006

[9]

W. Wu, C. Parmar, P. Grossmann, *et al.*

Exploratory study to identify radiomics classifiers for lung cancer histology

Front Oncol, 6 (2016), p. 71, 10.3389/fonc.2016.00071

[10]

S. Duffy, M. Farrell, K. McArdle, *et al.*

Novel methodology to replicate clot analogs with diverse composition in acute ischemic stroke

J Neurointerventional Surg, 9 (2017), pp. 486-491, 10.1136/neurintsurg-2016-012308

[11]

C. Rorden, H.-O. Karnath, L. Bonilha

Improving lesion-symptom mapping

J Cogn Neurosci, 19 (2007), pp. 1081-1088, 10.1162/jocn.2007.19.7.1081

[12]
J.J.M. Griethuysen, A. van Fedorov, C. Parmar, *et al.*
Computational radiomics system to decode the radiographic phenotype
Cancer Res, 77 (2017), pp. e104-e107, 10.1158/0008-5472.CAN-17-0339
[13]
J. Schindelin, I. Arganda-Carreras, E. Frise, *et al.*
Fiji: an open-source platform for biological-image analysis
Nat Methods, 9 (2012), pp. 676-682, 10.1038/nmeth.2019
[14]
R. Bourcier, R. Pautre, M. Mirza, *et al.*
MRI quantitative T2* mapping to predict dominant composition of in vitro thrombus
Am J Neuroradiol, 40 (2019), pp. 59-64, 10.3174/ajnr.A5938
[15]
S.D. Christiansen, J. Liu, M.B. Boffa, M. Drangova
Simultaneous R2* and quantitative susceptibility mapping measurement enables differentiation of thrombus hematocrit and age: an in vitro study at 3 T
J Neurointerventional Surg, 11 (2019), pp. 1155-1161, 10.1136/neurintsurg-2019-014802
[16]
S.K. Kim, W. Yoon, T.S. Kim, H.S. Kim, T.W. Heo, M.S. Park
Histologic analysis of retrieved clots in acute ischemic stroke: correlation with stroke etiology and gradient-echo MRI
Am J Neuroradiol, 36 (2015), pp. 1756-1762, 10.3174/ajnr.A4402
[17]
A.A.O. Carneiro, G.R. Vilela, D.B. de Araujo, O. Baffa
MRI relaxometry: methods and applications
Braz J Phys, 36 (2006), pp. 9-15, 10.1590/S0103-97332006000100005
[18]
G.M. Gunning, K. McArdle, M. Mirza, S. Duffy, M. Gilvarry, P.A. Brouwer
Clot friction variation with fibrin content; implications for resistance to thrombectomy
J Neurointerventional Surg, 10 (2018), pp. 34-38, 10.1136/neurintsurg-2016-012721
[19]
E. Laridan, F. Denorme, L. Desender, *et al.*
Neutrophil extracellular traps in ischemic stroke thrombi

Ann Neurol, 82 (2017), pp. 223-232, 10.1002/ana.24993
[20]
T. Boeckh-Behrens, M. Schubert, A. Förschler, *et al.*
The impact of histological clot composition in embolic stroke
Clin Neuroradiol, 26 (2016), pp. 189-197, 10.1007/s00062-014-0347-x
[21]
S. Duffy, R. McCarthy, M. Farrell, *et al.*
Per-Pass analysis of thrombus composition in patients with acute ischemic stroke undergoing mechanical thrombectomy
Stroke, 50 (2019), pp. 1156-1163, 10.1161/STROKEAHA.118.023419
[22]
O.V. Kim, R.I. Litvinov, M.S. Alber, J.W. Weisel
Quantitative structural mechanobiology of platelet-driven blood clot contraction
Nat Commun, 8 (2017), p. 1274, 10.1038/s41467-017-00885-x
View PDF
This article is free to access.
View in ScopusGoogle Scholar
[23]
D.B. Cines, T. Lebedeva, C. Nagaswami, *et al.*
Clot contraction: compression of erythrocytes into tightly packed polyhedra and redistribution of platelets and fibrin
Blood, 123 (2014), pp. 1596-1603, 10.1182/blood-2013-08-523860
[24]
V. Tutwiler, A.D. Peshkova, G. Le Minh, *et al.*
Blood clot contraction differentially modulates internal and external fibrinolysis
J Thromb Haemost, 17 (2019), pp. 361-370, 10.1111/jth.14370